Geochimica et Cosmochimica Acta Vol. 49, pp. 2323–2329

0016-7037/85/$3.00 + .00

A high pressure–high temperature study of TiO_2 solubility in Mg-rich phlogopite: implications to phlogopite chemistry

R. G. TRONNES,* A. D. EDGAR** and M. ARIMA

Department of Geology, University of Western Ontario, London, Ontario, Canada, N6A 5B7

(*Received February* 1, 1985; *accepted in revised form July* 29, 1985)

Abstract—The solubility of TiO_2 in phlogopites has been experimentally determined in the system $K_2Mg_6Al_2Si_6O_{20}(OH)_4$-$K_2Mg_4TiAl_2Si_6O_{20}(OH)_4$-$K_2Mg_5TiAl_4Si_4O_{20}(OH)_4$ between 825–1300°C and 10–30 kbar under vapour absent conditions. Starting compositions lie along the join $K_2Mg_6Al_2Si_6O_{20}(OH)_4$-$K_2Mg_{4.5}TiAl_3Si_5O_{20}(OH)_4$ which represents a combination of the $Mg^{[VI]}2Si^{[IV]} = Ti^{[VI]}2Al^{[IV]}$ and $2Mg^{[VI]} = Ti^{[VI]}\square^{[VI]}$ substitution mechanisms for Ti in phlogopites. The results of the experiments indicate a systematic increase in solubility of Ti with increasing temperature and decreasing pressure for given bulk TiO_2 content. Under isobaric conditions high temperature Ti-saturated phlogopite breaks down to Ti-deficient phlogopite + rutile + vapour. Mass balance calculations suggest that the vapour phase may contain K_2O dissolved in H_2O and that the reaction is controlled by the vapour phase. Analyses of phlogopites coexisting with rutile and vapour can be represented in terms of the end-member components phlogopite [$K_2Mg_6Al_2Si_6O_{20}(OH)_4$], eastonite [$K_2Mg_5Al_4Si_5O_{20}(OH)_4$], an octahedral site deficient Ti-phlogopite (Ti-OSD) of composition $K_2(Mg_4Ti\square)(Al_2Si_6)O_{20}(OH)_4$, and Ti-eastonite [$K_2Mg_5TiAl_4Si_4O_{20}(OH)_4$]. With decreasing amounts of Ti in these phlogopites there is a decrease in the Ti-eastonite component and increase in the eastonite component.

The general equation for the breakdown of Ti-phlogopite solid solution to Ti-free phlogopite + rutile + vapour is: 14 Ti-eastonite + 7 Ti-OSD $\rightleftharpoons$ 16 eastonite + 3 phlogopite + 21 rutile + 4 H_2O + 2 K_2O. Lack of knowledge of H_2O and K_2O activities in the vapour phase does not permit evaluation of thermodynamic constants for this reaction. The Ti solubility in phlogopites and hence its potential as a geothermobarometer under lower crustal to upper mantle conditions is likely controlled by common mantle minerals such as forsterite.

INTRODUCTION

PHLOGOPITE IS A common mineral in mantle and lower crustal rocks, particularly in ultrapotassic rocks, kimberlites, alkali basalts, lamproites, lamprophyres and granulites, and in xenoliths incorporated in these rocks. Mantle derived phlogopites have variable but often high TiO_2 contents which are related to their textural occurrences. High TiO_2 contents (>0.5 wt.%) are characteristic of secondary-textured phlogopites, whereas primary-textured phlogopites have lower TiO_2 (<0.5 wt.% (CARSWELL, 1975; DELANEY *et al.*, 1980).

In an experimental study on a single TiO_2-rich phlogopite composition [$K_2(Mg_4Ti)(Al_2Si_6)O_{20}(OH)_4$], FORBES and FLOWER (1974) showed that a phlogopite containing 9.6 wt.% TiO_2 was stable at 30 kbar and 1350°C in vapour (H_2O) present conditions, and up to 1475°C at the same pressure under vapour absent conditions. ROBERT (1976) showed that the solubility of TiO_2 in phlogopites increased with temperature and decreased with pressure in the range 600–1000°C and 1–7 kbar. These authors proposed different substitution mechanisms of Ti in the phlogopite structure. According to FORBES and FLOWER (1974), the mechanism was $2Mg^{[VI]} = Ti^{[VI]}\square^{[VI]}$ ($\square^{[VI]}$, vacant octahedral site) whereas ROBERT (1976) suggested $Mg^{[VI]}2Si^{[IV]} = Ti^{[VI]}2Al^{[IV]}$ as the likely substitution. High pressure experiments on rocks in which Ti-rich phlogopite crystallized as a suprasolidus mineral (EDGAR *et al.*, 1976; BARTON and HAMILTON, 1979) supported both proposed substitutions. Based on analyses of phlogopites from potassic-rich lavas, BARTON (1979) concluded that the type of Ti substitution in phlogopites was highly dependent on the bulk composition (particularly the Al) of the melt from which the phlogopite crystallized.

ARIMA and EDGAR (1981) examined phlogopites from mantle derived rocks and from phlogopites crystallized in high pressure experiments using ultrapotassic rock compositions. They concluded that the substitution was a combination of that proposed by FORBES and FLOWER (1974) and ROBERT (1976). Based on the phlogopites crystallized experimentally, ARIMA and EDGAR (1981) showed that the TiO_2 solubility increased with increasing temperature and fO_2 and probably decreased with increasing pressure, suggesting that the TiO_2-solubility in phlogopite might provide a useful geothermometer and possibly geobarometer.

In this study we determined the solubility of TiO_2 in phlogopites as a function of temperature and pressure in the system $K_2Mg_6Al_2Si_6O_{20}(OH)_4$-$K_2Mg_4TiAl_2Si_6O_{20}(OH)_4$-$K_2Mg_5TiAl_4Si_4O_{20}(OH)_4$ between 825–1300°C at 10–30 kbar. As shown in Fig. 1 the starting compositions were chosen along the join $K_2Mg_6Al_2Si_6O_{20}(OH)_4$-$K_2Mg_{4.5}TiAl_3Si_5O_{20}(OH)_4$. The join $K_2Mg_6Al_2Si_6O_{20}(OH)_4$-$K_2Mg_5TiAl_4Si_4O_{20}(OH)_4$ represents the substitution $Mg^{[VI]}2Si^{[IV]} = Ti^{[VI]}2Al^{[IV]}$ proposed by ROBERT (1976), whereas the join $K_2Mg_6Al_2Si_6O_{20}(OH)_4$-$K_2Mg_4TiAl_2Si_6O_{20}(OH)_4$ rep-

* Present address: Nordic Volcanological Institute, Geoscience Building, University of Iceland, 101 Reykjavek, Iceland.

** Offprint requests: A. D. Edgar.

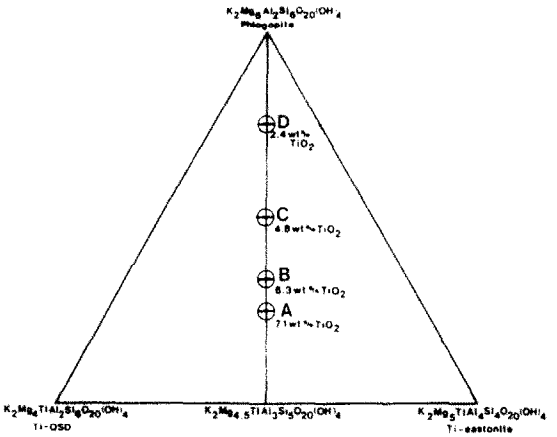

FIG. 1. Starting compositions along the join $K_2Mg_6Al_2Si_6O_{20}(OH)_4$-$K_2Mg_{4.5}TiAl_3Si_5O_{20}(OH)_4$ of the system phlogopite [$K_2Mg_6Al_2Si_6O_{20}(OH)_4$] - Ti-OSD[$K_2Mg_4TiAl_2Si_6O_{20}(OH)_4$]-Ti-eastonite[$K_2Mg_5TiAl_4Si_4O_{20}(OH)_4$] used in experimental study. TiO_2 content indicated next to each composition.

resents the substitution $2Mg^{[VI]} = Ti^{[VI]}\square^{[VI]}$ suggested by FORBES and FLOWER (1974). The compositions used represent substitutions intermediate between those proposed by ROBERT (1976) and by FORBES and FLOWER (1974).

STARTING MATERIALS, EXPERIMENTAL AND ANALYTICAL METHODS

Four phlogopite compositions, containing 2.4 to 7.1 wt.% TiO_2 (Fig. 1, A, B, C, D), were made from oxide mixtures. The starting materials consisted of Analar grade K_2CO_3, Al_2O_3, TiO_2 and MgO; and SiO_2 as 99.9% pure quartz. Each oxide was dried at 1000°C and K_2CO_3 was heated at 110°C, to remove absorbed H_2O, prior to weighing. The mixture was ground and heated to 950°C for 30 min to convert K_2CO_3 to K_2O followed by grinding and sintering at 1050°C for 30 min. The appropriate weight of deionized H_2O was added to each starting composition as required by the formula. The justification of adding this amount of H_2O assumes that coupled substitutions between Ti and (OH) are probably unimportant (ARIMA and EDGAR, 1981). Microprobe analyses of phlogopites in high pressure experiments in which phlogopite was the only phase gave results in accordance with that of the starting material.

All experiments were performed with a 1.27 cm diameter piston cylinder apparatus using the "hot piston out" technique and graphite furnaces (BOYD and ENGLAND, 1960). Talc-pyrex glass was used as a pressure transmitting medium for most runs, except a few at 10 kbar in which talc-boron nitride was the medium. Pressures and temperatures were calibrated with the kyanite = sillimanite transition at 22 kbar and 1300°C (RICHARDSON *et al.*, 1968), with the albite = jadeite + quartz at 16.3 kbar and 600°C (JOHANNES *et al.*, 1971; HOLLAND, 1980) and with the melting point of diopside at 10 kbar and 1530°C (BOYD and ENGLAND, 1960). Pressures and temperatures were within ±0.5 kbar and ±10°C respectively of the accepted values of these calibrants. No friction correction was made for pressure and no pressure correction was made to the e.m.f. of the Pt-$Pt_{90}Rh_{10}$ thermocouples. For the durations of the runs (5–16 hours), no deterioration was observed in these thermocouples.

Runs were done in 7 × 1 mm Pt capsules closed at each end by arc welding. Within each capsule 6 mg of the anhydrous starting material and 0.27 mg of deionized H_2O were added by microsyringe. Weighing errors in the addition of the H_2O did not exceed ±10% of the amount required, based on repeated weighings. At the end of each run the capsules were weighed prior to opening. In experiments in which the products were phlogopite or phlogopite + rutile, no weight loss was observed relative to the "before run" weight. In experiments in which a weight difference was observed the products consisted of forsterite and kalsilite in addition to phlogopite and rutile. These runs were discarded. In runs yielding only phlogopite, there was no evidence of a free vapour phase but we cannot demonstrate that traces of vapour were not present. In runs with phlogopite + rutile, mass balance calculations (p. 9–11) show that very small amounts of vapour must be present. For some of these runs, the phlogopite grains appeared to contain small fluid inclusions(?); a phenomenon not observed in runs consisting only of phlogopite.

Identification of the products of the experiments was made by optical observation in grain mounts and in polished thin sections. Phlogopite occurs as hexagonal-shaped plates, 10–100 μm; and rutile as tiny, high relief grains readily identifiable even in small amounts. No other phases were detected. Analyses of the phlogopite were done with a MAC-400 automated electron microprobe using 15 kV and a sample current of 150 μA.

REVERSAL EXPERIMENTS

The experiments are believed to represent equilibrium, based on isobarically reversed runs across the solubility line using composition B (Table 1, Fig. 2). A run within the phlogopite + rutile + vapour field was kept at 20 kbar and 1080°C for 6 hours before raising the temperature to 1150°C. After a further 6 hours, the run gave single phase phlogopite containing 6.3 wt.% TiO_2. A further run was held at the same pressure and 1150°C for 6 hours before the temperature was lowered to 1080°C at the same pressure. After 6 hours this run produced phlogopite + rutile + vapour; the phlogopite containing 5.8 wt.% TiO_2. The TiO_2 contents of the phlogopites in these reversal experiments were very comparable to those in non-reversed runs (Table 1, Fig. 2).

Similar reversals were performed at 25 kbar between 1100°C and 1150°C. These runs resulted in assemblages identical to those of non-reversed runs at these temperatures and had comparable TiO_2 contents in the phlogopites (Table 1).

RESULTS

Results of the experiments are plotted on Fig. 2 and analyses of the phlogopites are given in Table 1. The lines on Fig. 2 represent the P-T conditions separating the single phase phlogopite and the three phase phlogopite + rutile + vapour fields. The positive P-T slopes of these lines indicate that for each bulk composition the solubility of TiO_2 in phlogopite increases with temperature and decreases with pressure. The analyses of phlogopites coexisting with rutile + vapour indicate a systematic increase in TiO_2 content of phlogopite with increasing temperature at constant pressure and with decreasing pressure at constant temperature (Table 1, Fig. 2). Although the results are most complete for composition B, the data for the other compositions clearly exhibit the same tendencies (Fig. 2).

MASS BALANCE CALCULATIONS OF RUN PRODUCTS

Based on the experimental results (Table 1, Fig. 2), the incorporation of TiO_2 in phlogopites involves the reaction:

$$\text{phlogopite}^{I} \rightleftharpoons \text{phlogopite}^{II} + \text{rutile} + \text{vapour} \quad (1)$$

in which phlogopite[I] = single phase phlogopite containing the same amounts of TiO_2 and other components as the starting material (Table 1); phlogopite[II] = a phlogopite containing lower TiO_2 than phlogopite[I]; the amounts of TiO_2 depending on the P, T and wt.% TiO_2 in the bulk composition used (Table 1). Assuming phlogopite is the only H_2O-bearing mineral present, a vapour phase must coexist with phlogopite[II] and rutile.

In theory, there are many reactions involving combinations of forsterite, enstatite, kalsilite, leucite, sanidine, and geikielite ($MgTiO_3$) along with phlogopite and rutile which might explain the solubility of TiO_2 in phlogopite. Although the products of all runs were carefully examined optically and by electron microprobe, there was no indication of any of these solid phases or of glass being present. The only indication *from the experiments* of a vapour phase being present is the presence of what may be fluid inclusions in phlogopites coexisting with rutile.

Inability to identify solid phases other than phlogopite and rutile in the experiments does not preclude their presence in very minor amounts. To determine whether these minor phases were present and to establish the reaction involved in the incorporation of TiO_2 in phlogopite, least squares mass balance calculations (STORMER and NICHOLLS, 1978) were done for all the experiments using the averages of analyses of single phase phlogopite (phlogopite[I]) and of the phlogopite coexisting with rutile (phlogopite[II]). The general equation can be written as:

$$100\%\ \text{phlogopite}^{I} = x\ \text{phlogopite}^{II} + \underset{\text{(rutile)}}{yTiO_2} + \underset{\text{(vapour)}}{z_1K_2O + z_2H_2O}. \quad (2)$$

Table 2 gives results of these calculations for runs on each bulk composition with the minimum TiO_2 in phlogopite[II] (Fig. 2) in experiments at highest pressures and lowest temperatures. These calculations confirm that the amount of vapour ($z_1 + z_2$) is small. The small residuals in all calculations probably reflect analytical error. The absence of systematic relations in the residuals strongly implies that no other mineral phases are involved in the reaction. It is possible however that the vapour phase may contain some K_2O.

These calculations show that the mechanism of Ti incorporation in phlogopites in our experiments is controlled by H_2O activity. The amount of H_2O added represents the minimum required to produce this reaction. Lower $a_{(H_2O)}$ would result in anhydrous phases (*e.g.*, forsterite, etc.) coexisting with phlogopite[I] whereas higher $a_{(H_2O)}$ might change the positions of the solubility lines (Fig. 2).

THE PROPORTIONS OF END-MEMBER PHLOGOPITE COMPONENTS

The incorporation of TiO_2 in phlogopite can be represented in terms of end-member components calculated from the structural formula. Appendix 1 outlines the procedure for this calculation. The following components are chosen to represent the compositions of the experimentally produced phlogopites:

1. Phlogopite, $K_2Mg_6(Al_2Si_6)O_{20}(OH)_4$
2. Ti-OSD component (where OSD:octahedral site deficiency), $K_2(Mg_4Ti\square)(Al_2Si_6)O_{20}(OH)_4$, representing the substitution $2Mg \rightleftharpoons Ti\square$
3. Ti-eastonite, $K_2(Mg_5Ti)(Al_4Si_4)O_{20}(OH)_4$, representing the substitution $Mg2Si \rightleftharpoons Ti2Al$
4. Eastonite, $K_2(Mg_5Al)(Al_3Si_5)O_{20}(OH)_4$, representing the substitution $MgSi \rightleftharpoons Al^{[VI]}Al^{[IV]}$
5. Talc (interlayer site deficiency) component, $\square_2Mg_6Si_8O_{20}(OH)_4$, representing the substitution $KAl \rightleftharpoons \square Si$.

The starting compositions can be represented in terms of only three of these end-member components—phlogopite, Ti-OSD and Ti-eastonite. As shown in Fig. 1, each of these compositions contains equal ratios of Ti-OSD and Ti-eastonite but varying proportions of phlogopite. The single phase phlogopites crystallized in the experiments are similar in composition to that of the starting material but have small amounts of eastonite and talc components (Table 1, Fig. 3). Most of the discrepancies between the single phase phlogopites and the starting compositions may be due to systematic analytical errors.

As the TiO_2 content of the phlogopites coexisting with rutile and vapour decreases, there is an increase in eastonite and decrease in Ti-eastonite components (Table 1, Figs. 3 and 4). The change in the Ti-OSD component is much smaller, but appears to decrease slightly with decreasing TiO_2 content of the phlogopite (Figs. 3 and 4).

Table 1 indicates that the changes in the proportions of the Ti-eastonite component between the single phase phlogopite and the phlogopite coexisting with rutile and vapour are negatively correlated with changes in the proportions of the eastonite component. The Ti-OSD component is generally lower in the phlogopites coexisting with rutile and vapour than in the single phase compositions.

REACTION INVOLVED IN TiO_2 SOLUBILITY IN PHLOGOPITE

Using these relationships and the results of the mass balance calculations, the following reaction for the complete breakdown of single phase phlogopite of composition B to phlogopite + rutile + vapour is:

$$\underbrace{14\ \text{Ti-eastonite} + 14\ \text{Ti-OSD} + 14\ \text{phlogopite}}_{\text{phlogopite}^{I}\ \text{ss}} \rightleftharpoons \underbrace{16\ \text{eastonite} + 17\ \text{phlogopite} + 7\ \text{Ti-OSD}}_{\text{phlogoite}^{II}\ \text{ss}} + \underbrace{21\ TiO_2}_{\text{rutile}} + \underbrace{4\ H_2O + 2\ K_2O}_{\text{vapour}}. \quad (3)$$

Eqn. (3) can be reduced to:

Table 1. Experimental results and analyses of phlogopites.

Composition	A	A	A	A	A	A	A	A	A	A
Pressure(kbar)	10	15	20	30	15	30	10	15	15	30
Temperature(°C)	1000	1000	1000	1000	1100	1100	1150	1150	1175	1200
Run time (hrs)	6.5	7.5	6	6.5	6	8	6	6	8	7.5
Coexisting phase	Ru	Ru	Ru	Ru	Ru	Ru	-	Ru	-	Ru
SiO_2	37.4	38.3	39.3	39.2	40.8	39.1	37.6	38.4	38.9	39.0
Al_2O_3	16.8	17.5	17.4	16.6	14.1	17.4	16.6	17.7	16.6	17.1
TiO_2	6.7	6.0	4.2	3.6	6.1	3.8	7.1	6.3	7.3	4.7
MgO	23.7	23.2	23.3	23.3	23.8	24.7	23.3	23.2	22.9	23.4
K_2O	11.1	10.7	10.5	10.7	11.0	11.1	11.0	10.7	10.6	10.8
Sum	95.7	95.7	94.7	93.4	95.8	96.1	95.6	96.3	96.3	95.0
Si	5.241	5.334	5.504	5.577	5.678	5.429	5.264	5.322	5.382	5.459
Al	2.759	2.666	2.496	2.423	2.311	2.571	2.736	2.678	2.618	2.541
Al[1]	0.018	0.209	0.378	0.356	[0.011]	0.270	0.014	0.206	0.088	0.276
Ti	0.705	0.629	0.442	0.383	0.625	0.399	0.746	0.652	0.762	0.497
Mg	4.953	4.806	4.857	4.939	4.934	5.105	4.874	4.781	4.714	4.895
OSO	5.676	5.644	5.677	5.678	5.559	5.774	5.634	5.639	5.564	5.668
K	1.976	1.908	1.879	1.946	1.944	1.955	1.962	1.889	1.876	1.934
Ti-OSO	32.2	34.6	30.8	30.8	44.1	21.9	36.6	35.1	43.1	32.1
Ti-eastonite	38.1	26.7	11.4	5.8	18.5	16.8	37.9	28.4	32.3	16.0
Phlogopite	26.4	11.2	11.4	22.4	34.5	29.9	22.1	8.4	8.6	18.7
Eastonite[2]	2.1	23.0	40.6	38.4	[0.2]	29.3	1.5	22.6	9.8	30.0
Talc	1.2	4.5	5.8	2.6	2.8	2.2	1.9	5.4	6.1	3.2

Composition	A	A	B	B	B	B	B	B	B	B	B(r)
Pressure(kbar)	25	30	10	15	20	25	30	15	25	30	20
Temperature(°C)	1250	1275	1000	1000	1000	1000	1000	1070	1070	1070	1150-1080
Run time (hrs)	6	6	9	10.5	7	6	6	10.5	6	6	6+6
Coexisting phase	-	-	Ru	Ru	Ru	Ru	Ru	-	Ru	Ru	Ru
SiO_2	37.9	38.4	37.7	38.2	39.0	39.7	39.8	37.9	37.8	39.5	38.5
Al_2O_3	17.0	16.3	16.5	16.5	16.5	17.2	16.9	16.2	16.2	17.5	16.4
TiO_2	7.1	7.2	5.6	5.1	4.4	4.5	3.0	6.3	5.2	4.1	5.8
MgO	23.3	23.3	24.1	23.6	24.0	23.7	24.4	23.5	24.1	23.9	24.5
K_2O	10.5	10.5	10.6	10.8	11.1	10.9	11.2	11.0	10.7	10.7	11.5
Sum	95.8	95.7	94.5	94.2	95.0	96.0	95.3	94.9	94.0	95.7	96.7
Si	5.279	5.347	5.331	5.413	5.476	5.500	5.557	5.349	5.375	5.480	5.344
Al	2.721	2.653	2.669	2.587	2.524	2.500	2.443	2.651	2.625	2.520	2.656
Al[1]	0.068	0.027	0.072	0.161	0.202	0.300	0.342	0.039	0.088	0.340	0.021
Ti	0.741	0.758	0.596	0.584	0.466	0.473	0.313	0.669	0.551	0.430	0.602
Mg	4.840	4.838	5.075	4.981	5.036	4.892	5.086	4.939	5.105	4.942	5.074
OSO	5.649	5.623	5.743	5.726	5.704	5.665	5.741	5.647	5.744	5.712	5.697
K	1.872	1.863	1.917	1.950	1.981	1.926	1.994	1.980	1.947	1.896	2.040
Ti-OSO	34.8	37.5	25.4	30.4	28.8	32.4	24.9	35.3	25.3	27.6	29.7
Ti-eastonite	38.8	38.0	33.7	23.3	16.6	13.2	5.1	31.6	29.2	13.6	29.1
Phlogopite	12.5	14.6	28.8	26.1	22.2	18.4	32.9	28.2	33.1	17.1	38.9
Eastonite[2]	7.6	3.1	8.0	17.8	31.4	32.5	36.8	3.9	9.8	36.7	2.3
Talc	6.4	6.8	4.1	2.4	0.9	3.5	0.3	1.0	2.6	5.0	-

Composition	B	B(r)	B	B(r)	B	B(r)	B	B	B	B	B	B
Pressure(kbar)	20	25	20	20	25	25	30	20	30	30	25	30
Temperature(°C)	1100	1150-1100	1150	1080-1150	1150	1100-1150	1150	1200	1200	1215	1225	1225
Run time (hrs)	16	6+6	6	6+6	7	6+6	6	7	5	8	7	6
Coexisting phase	Ru	Ru	-	-	-	-	Ru	-	-	-	-	-
SiO_2	37.2	39.7	37.5	40.9	38.4	38.9	38.2	38.3	37.9	39.0	39.0	38.1
Al_2O_3	17.7	17.6	17.0	15.3	16.5	16.3	15.8	16.4	16.3	16.1	16.1	16.7
TiO_2	6.0	5.0	6.3	6.2	6.3	6.1	5.7	6.1	6.1	6.2	6.2	6.1
MgO	23.8	24.6	23.9	23.3	23.6	23.5	25.1	24.0	23.5	23.5	23.6	23.9
K_2O	10.7	10.9	10.8	10.6	11.0	10.5	10.8	10.8	10.9	10.7	10.6	10.7
Sum	95.4	97.8	95.5	96.3	95.8	95.3	95.6	95.6	94.7	95.5	95.5	95.5
Si	5.209	5.402	5.249	5.635	5.360	5.433	5.350	5.357	5.355	5.452	5.437	5.326
Al	2.791	2.598	2.751	2.365	2.640	2.567	2.605	2.643	2.645	2.548	2.563	2.674
Al[1]	0.138	0.222	0.058	0.120	0.077	0.116	[0.045]	0.054	0.062	0.098	0.082	0.070
Ti	0.628	0.515	0.666	0.642	0.663	0.641	0.554	0.641	0.649	0.646	0.654	0.646
Mg	4.987	4.994	4.987	4.786	4.902	4.893	5.231	5.000	4.953	4.884	4.904	4.985
OSO	5.744	5.731	5.711	5.548	5.642	5.650	5.785	5.695	5.664	5.628	5.640	5.701
K	1.908	1.884	1.938	1.863	1.952	1.871	1.952	1.920	1.955	1.902	1.892	1.909
Ti-OSO	25.2	26.2	28.6	45.1	35.4	35.1	21.0	30.4	33.3	36.8	35.6	29.6
Ti-eastonite	36.6	23.9	37.5	19.1	30.2	29.0	34.8	33.3	31.1	27.1	29.2	34.4
Phlogopite	18.4	19.9	24.3	17.0	23.3	17.9	39.7	26.4	26.4	20.4	20.8	23.6
Eastonite[2]	15.3	24.3	6.5	12.0	8.6	11.6	[0.8]	6.0	7.0	10.9	9.1	7.9
Talc	4.5	5.6	3.1	6.9	2.4	6.5	3.8	4.0	2.2	4.9	5.3	4.5

Table 1. Cont.

Composition	C	C	C	C	C	C	D	D	D	D	D	D
Pressure(kbar)	10	10	10	15	20	30	15	20	25	30	15	30
Temperature(°C)	850	900	950	950	950	950	825	825	825	825	900	900
Run time (hrs)	10	12	8	8	10	10	20	12	12	12	13	12
Coexisting phase	Ru	Ru	-	Ru	Ru	Ru	Ru	Ru	Ru	Ru	-	Ru
SiO_2	40.0	39.8	39.4	39.7	40.0	40.1	41.4	42.0	42.2	42.5	40.8	39.6
Al_2O_3	15.7	15.7	15.1	15.5	15.5	16.5	14.0	13.7	13.8	13.7	13.9	15.8
TiO_2	4.1	4.3	4.8	4.5	4.1	2.6	1.1	0.6	0.4	0.3	2.1	0.8
MgO	24.3	25.1	25.1	24.7	24.6	25.3	27.2	27.4	27.6	27.6	27.6	26.8
K_2O	11.2	11.1	10.8	11.2	10.9	10.8	10.0	10.8	11.0	10.8	11.0	10.3
Sum	95.3	96.0	95.2	95.6	95.1	95.3	93.7	94.5	93.2	94.9	95.4	93.3
Si	5.595	5.529	5.521	5.543	5.604	5.583	5.832	5.891	5.896	5.927	5.697	5.629
Al	2.405	2.471	2.479	2.457	2.396	2.417	2.168	2.109	2.104	2.073	2.289	2.371
Al[1]	0.180	0.107	0.014	0.091	0.152	0.295	0.152	0.151	0.169	0.182	[0.014]	0.277
Ti	0.436	0.447	0.501	0.477	0.433	0.276	0.117	0.065	0.041	0.031	0.207	0.081
Mg	5.065	5.198	5.252	5.139	5.128	5.250	5.724	5.733	5.738	5.736	5.754	5.676
OSO	5.681	5.753	5.767	5.707	5.713	5.821	5.993	5.949	5.948	5.949	5.961	6.034
K	1.991	1.965	1.930	1.997	1.952	1.927	1.796	1.929	1.958	1.930	1.954	1.864
Ti-OSD	31.2	24.4	23.3	28.9	28.1	17.2	0.7	5.0	4.1	3.1	3.8	-
Ti-eastonite	11.4	19.7	26.7	18.2	14.3	9.4	10.8	1.5	-	-	16.9	8.1
Phlogopite	37.1	42.2	45.0	42.5	38.3	37.9	61.7	73.5	76.9	75.2	76.8	57.6
Eastonite[2]	19.8	11.9	1.5	10.1	16.8	32.0	16.8	16.6	16.9	18.2	[0.2]	27.5
Talc	0.4	1.8	3.5	0.2	2.4	3.5	10.0	3.5	2.1	3.5	2.3	6.8

Composition	D	D	D	D
Pressure(kbar)	15	15	20	30
Temperature(°C)	950	1000	1000	1000
Run time (hrs)	13	6	6	10
Coexisting phase	-	-	-	Ru
SiO_2	40.6	40.7	41.0	41.2
Al_2O_3	13.6	14.1	13.8	13.9
TiO_2	2.1	2.3	2.4	1.3
MgO	27.3	26.7	26.5	28.1
K_2O	11.0	10.6	10.8	11.4
Sum	94.6	94.4	94.7	95.9
Si	5.730	5.732	5.769	5.733
Al	2.253	2.268	2.231	2.267
Al[1]	[0.017]	0.073	0.056	0.019
Ti	0.202	0.242	0.258	0.136
Mg	5.737	5.592	5.550	5.819
OSO	5.939	5.907	5.864	5.974
K	1.971	1.897	1.930	2.027
Ti-OSD	5.9	9.2	13.5	2.6
Ti-eastonite	14.3	14.8	12.2	10.8
Phlogopite	78.0	62.8	64.6	84.4
Eastonite[2]	[0.3]	8.1	6.2	2.2
Talc	1.5	5.1	3.5	-

The calculation of structural formulae (22 O-atoms) and end member molecules is given in the Appendix. [1]: Numbers in brackets represent tetrahedral Ti when no octahedral Al is present. [2]: Numbers in bracket represent the tetrahedral Ti molecule when no eastonite is present. Coexisting phase: Rutile (Ru). Reversed experiments are indicated as (r), and both the initial and final temperatures are given.

$$\underbrace{14\ \text{Ti-eastonite} + 7\ \text{Ti-OSD}}_{\text{phlogopite}^{1}\ \text{ss}} \rightleftharpoons \underbrace{16\ \text{eastonite} + 3\ \text{phlogopite}}_{\text{phlogopite}^{11}\ \text{ss}} + 21\ TiO_2 + \underbrace{4\ H_2O + 2\ K_2O}_{\text{vapour}}. \quad (4)$$

(rutile)

This is the general equation which links the end-member components in the phlogopite solid solution and is in agreement with the overall trend of the experimental results (Table 1, Figs. 3 and 4).

The equilibrium constant for the reaction is:

$$K = \frac{(a_{\text{Ea}}^{\text{phlog}})^{16} \cdot (a_{\text{Ph}}^{\text{phlog}})^{3}}{(a_{\text{Ti-ea}}^{\text{phlog}})^{14} \cdot (a_{\text{Ti-OSD}}^{\text{phlog}})^{7}} \cdot (a_{TiO_2}^{\text{rut}})^{21} \cdot (a_{H_2O}^{\text{vap}})^{4} \cdot (a_{K_2O}^{\text{vap}})^{2} \quad (5)$$

where a_i^j is the activity of component i in phase j. If the activities of solid phases are equal to the molar proportions of the components in each of the phases this expression reduces to:

$$K = C\,\frac{(X_{\text{Ea}})^{16} \cdot (X_{\text{Ph}})^{3}}{(X_{\text{Ti-ea}})^{14} \cdot (X_{\text{Ti-OSD}})^{7}} = C \cdot k \quad (6)$$

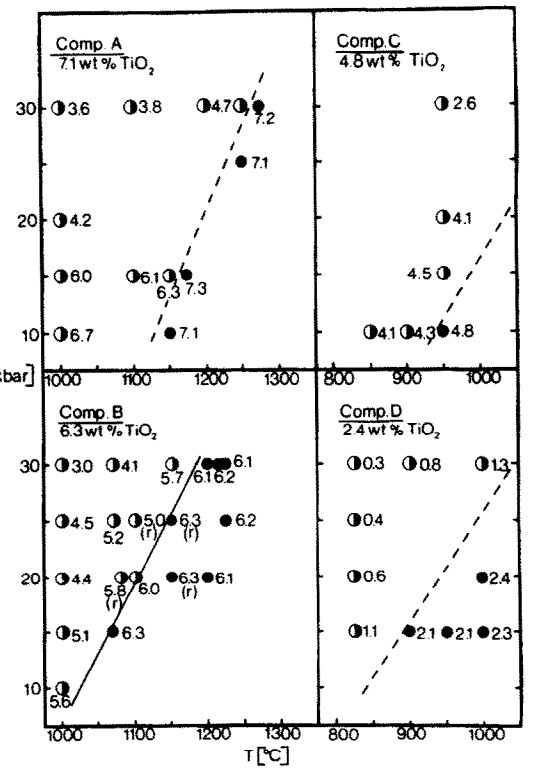

FIG. 2. *P-T* relationships for each starting composition given in Fig. 1. Continuous line indicates limit of solubility of TiO_2 for composition B; dashed lines are approximate solubility limits of TiO_2 for compositions A, C, and D. Half filled circles represent phlogopite + rutile + vapour runs, filled circles are single phase phlogopite. Numbers adjacent to each run are wt.% TiO_2 in phlogopite. Reversed runs are indicated by (*r*) (Table 1).

Table 2. Selected results from mass balance calculation (FORTRAN-program by Stormer and Nicholls, 1978).

100 wt. % Phlogopite[1] → X wt. % Phlogopite[11] (single phase)
+ Y wt. % TiO_2 (rutile) + Z_1 wt. % K_2O + Z_2 wt. % H_2O (vapour)

All calculations for 30 kbar runs

Single phase phlogopite[1] (average composition)	A	B	C	D
Phlogopite[11] (T°C)	1000	1000	950	825
X (wt. %)	95.91	96.46	97.60	97.32
Y (wt. %)	3.69	3.34	2.19	2.02
Z_1 (wt. %)	0.17	0.02	0.19	0.46
Z_2 (wt. %)	0.24	0.18	0.02	0.20
Residuals:				
SiO_2	0.46	0.15	-0.31	0.50
Al_2O_3	-0.46	-0.07	0.99	-0.55
TiO_2	0.07	0.02	-0.08	0.09
MgO	-0.22	-0.13	-0.44	-0.23
K_2O	0.07	0.02	-0.08	0.09
H_2O	0.07	0.02	-0.08	0.09

where $C = a^4_{(H_2O)} \cdot a^2_{(K_2O)}$. The K in Eqn. (6) is a function of the P, T and bulk composition of the system. Since the term C in Eqn. (6) includes $a_{(H_2O)}$ and $a_{(K_2O)}$ in the vapour phase, K cannot be determined and thermodynamic parameters, $\Delta\bar{H}$, $\Delta\bar{S}$ and $\Delta\bar{V}$ for the reaction cannot be estimated. However, the term k in this equation may reflect the behavior of the term K. Using the limited data available, ln k has been plotted against pressure for given bulk compositions and temperatures in Fig. 5; Fig. 5 shows an increase in ln k with increasing pressure for all compositions. There is also a suggestion that ln k decreases with increasing temperature at constant pressure. We cannot assess the effect of the bulk TiO_2 in the system based on the ln k values. However, as shown in Fig. 2, the solubility of TiO_2 in phlogopites is clearly a function of the bulk composition of the system.

TiO_2 SOLUBILITY IN PHLOGOPITE AS A POTENTIAL GEOTHERMOBAROMETER

The dependence of the solubility of TiO_2 in phlogopites on pressure and temperature as shown by this study makes TiO_2 solubility in phlogopites in nature a potential geothermobarometer. In this study the TiO_2 solubility was controlled by the H_2O content of the vapour which is the minimum required to produce single phase phlogopites. Under upper mantle and

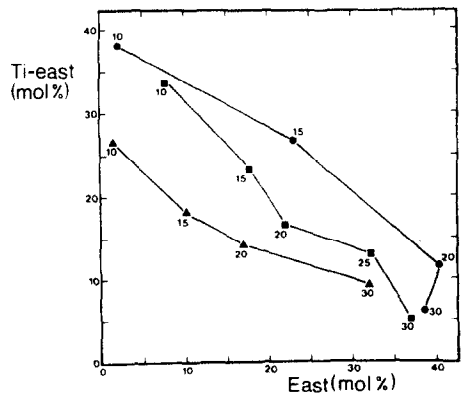

FIG. 3. Ti-eastonite *vs.* eastonite. Circles—composition A, 1000°C; squares—composition B, 1000°C; triangles—composition C, 950°C. Pressures are indicated next to each data point.

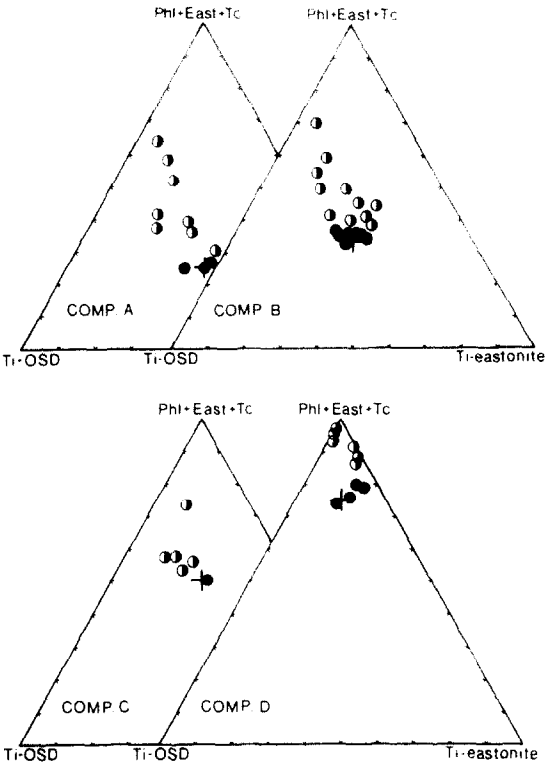

FIG. 4. Compositions of phlogopites plotted in the system (phlogopite + eastonite + talc)-(Ti-OSD)-(Ti-eastonite). Crosses represent starting compositions (Fig. 1). Other symbols as in Fig. 2.

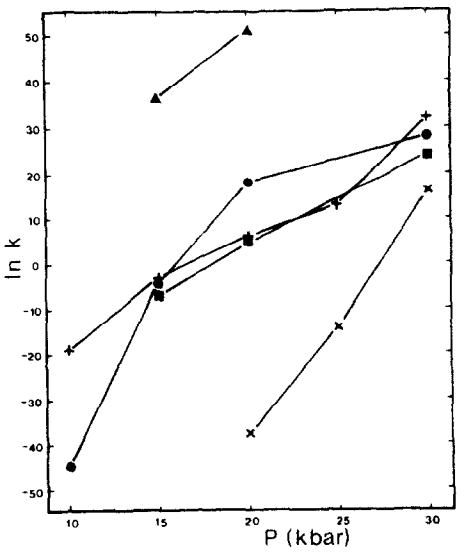

FIG. 5. ln k *vs.* P for various constant T conditions. Filled circles—composition A, 1000°C; +—composition B, 1000°C; ■—composition C, 950°C, ×—composition B, 1080°C; ▲—composition D, 825°C.

lower crustal conditions, the solubility of TiO_2 in phlogopite is likely buffered by coexisting mineral phases such as olivine. Based on our experiments and on the postulated end-member components of the Ti-bearing phlogopites, a simplified reaction controlling TiO_2 solubility in rocks in the upper mantle and lower crust may be:

$$\underset{\text{Ti-eastonite}}{K_2Mg_5TiAl_4Si_4O_{20}(OH)_4} + \underset{\text{Ti-OSD}}{K_2Mg_4TiAl_2Si_6O_{20}(OH)_4} + \underset{\text{Forsterite}}{Mg_2SiO_4} \rightleftharpoons \underset{\text{phlogopite}}{K_2Mg_6Al_2Si_6O_{20}(OH)_4} + \underset{\text{eastonite}}{K_2Mg_5Al_4Si_5O_{20}(OH)_4} + 2\,\underset{\text{rutile}}{TiO_2}. \quad (7)$$

Other common upper mantle-lower crustal minerals may control the TiO_2 solubility in phlogopites. Experimental investigation of systems containing such mineral species are required before the potential of the TiO_2 content of phlogopite can be quantitatively assessed as a geothermobarometer. The present results show that TiO_2 solubility in phlogopite may indeed prove a useful geothermobarometer. The incorporation of Ti in phlogopite by the substitution Mg2Si $\rightleftharpoons$ Ti2Al is pressure sensitive and therefore a potentially valuable geobarometer.

Acknowledgements—This study was supported by fellowships from Norges Teknisk-Naturvitenskapelige Forskningsråd to R.G.T. and by an operating grant from the Natural Sciences and Engineering Research Council of Canada to A.D.E. Technical assistance was provided by R. Shirran, J. Forth, S. Talman and R. L. Barnett.

Editorial handling: J. M. Ferry

REFERENCES

ARIMA M. and EDGAR A. D. (1981) Substitution mechanisms and solubility of titanium in phlogopites from rocks of probable mantle origin. *Contrib. Mineral. Petrol.* **77**, 288–295.

BARTON M. (1979) A comparative study of some minerals occurring in the potassium-rich alkaline rocks of the Leucite Hills, Wyoming, the Vico volcano, Western Italy, and the Toro-Ankole region, Uganda. *N. Jb. Mineral. Abh.* **137**, 113–134.

BARTON M. and HAMILTON D. L. (1979) The melting relationships of a madupite from the Leucite Hills, Wyoming, to 30 Kb. *Contrib. Mineral. Petrol.* **69**, 133–142.

BOYD F. R. and ENGLAND J. L. (1960) Apparatus for phase equilibrium measurements at pressure up to 50 Kb and temperatures to 1750°C. *J. Geophys. Res.* **65**, 741–748.

CARSWELL D. A. (1975) Primary and secondary phlogopites and clinopyroxenes in garnet lherzolite xenoliths. *Phys. Chem. Earth* **9**, 417–429.

DELANEY J. S., SMITH J. V., CARSWELL D. A. and DAWSON J. B. (1980) Chemistry of micas from kimberlites and xenoliths—II. Primary- and secondary-textured micas from peridotite xenoliths. *Geochim. Cosmochim. Acta* **44**, 857–872.

EDGAR A. D., GREEN D. H. and HIBBERSON W. O. (1976) Experimental petrology of a highly potassic magma. *J. Petrol.* **17**, 339–356.

FORBES W. C. and FLOWER M. F. J. (1974) Phase relations of titan-phlogopite, $K_2Mg_4TiAl_2Si_4O_{20}(OH)_4$: a refractory in the upper mantle? *Earth Planet. Sci. Lett.* **22**, 60–66.

HOLLAND T. J. B. (1980) The reaction albite = jadeite + quartz determined experimentally in the range 600°C–1200°C. *Amer. Mineral.* **65**, 129–134.

JOHANNES W., BELL P. M., MAO H. K., BOETTCHER A. L., CHIPMAN D. W., HAYS J. F., NEWTON R. C. and SEIFERT F. (1971) An interlaboratory comparison of piston-cylinder pressure calibration using the albite-breakdown reaction. *Contrib. Mineral. Petrol.* **32**, 24–38.

RICHARDSON S. W., BELL P. and GILBERT M. C. (1968) Kyanite-sillimanite equilibrium between 700 and 1500°C. *Amer. J. Sci.* **266**, 513–541.

ROBERT J. L. (1976) Titanium solubility in synthetic phlogopite solid solutions. *Chem. Geol.* **17**, 213–227.

STORMER J. C. and NICHOLLS J. (1978) XLFRAC: a program for the interactive testing of magmatic differentiation models. *Computers and Geosciences* **4**, 143–159.

APPENDIX 1

Calculation of end-member components of phlogopites

The molecular proportions of the end-member components were calculated from the structural formula (O = 22) in the following sequence:

1. Octahedral Al was combined with K, Mg, and Si to form eastonite $[K_2(Mg_5Al)(Al_3Si_5)O_{22}]$.
2. A talc component, $\square_2Mg_6Si_8O_{20}(OH)_4$, was formed from the interlayer site deficiency (ISD = 2-K).
3. Since both the Ti-OSD and the phlogopite components have Al/Si ratios of 1/3, whereas the Ti-eastonite component has an Al/Si ratio of 1, the following relations can be established (N_i^j is the amount of cation i in component j):

$$N_{Si}^{\text{Ti-east}} = N_{Al}^{\text{Ti-east}},\ N_{Si}^{\text{Ti-OSD}} = 3N_{Al}^{\text{Ti-OSD}},$$
$$N_{Si}^{\text{Phlog}} = 3N_{Al}^{\text{Phlog}} \quad \text{(A1)}$$

$$\Sigma N_{Si} = N_{Si}^{\text{Ti-east}} + N_{Si}^{\text{Ti-OSD}} + N_{Si}^{\text{Phlog}} \quad \text{(A2)}$$

$$\Sigma N_{Al} = N_{Al}^{\text{Ti-east}} + N_{Al}^{\text{Ti-OSD}} + N_{Al}^{\text{Phlog}} \quad \text{(A3)}$$

Combining equations (A1) and (A2) gives:

$$\Sigma N_{Si} = N_{Al}^{\text{Ti-east}} + 3(N_{Al}^{\text{Ti-OSD}} + N_{Al}^{\text{Phlog}}),$$

and inserting Eqn. (A3):

$$\Sigma N_{Si} = N_{Al}^{\text{Ti-east}} + 3(\Sigma N_{Al} - N_{Al}^{\text{Ti-east}})$$

$$N_{Al}^{\text{Ti-east}} = 1/2[3(\Sigma N_{Al} - \Sigma N_{Si})]. \quad \text{(A4)}$$

The Ti-eastonite molecule, $K_2Mg_5TiAl_4Si_4O_{20}(OH)_4$, was formed from the amount of Al derived from Eqn. (A4) along with the required K, Mg, Ti and Si. This procedure adjusts the Al/Si ratio to 1/3 for the remaining Ti-OSD and phlogopite components.

4. The remaining Ti after step 3 is equal to the octahedral site deficiency (6-sum of octahedral cations). The Ti-OSD component, $K_2Mg_4TiAl_2Si_6O_{20}(OH)_4$ was formed by combining the remaining Ti with the required K, Mg, Al and Si.
5. The remaining cations are now present in proportions identical to the stoichiometric cation ratios of the phlogopite component, $K_2Mg_6Al_2Si_6O_{20}(OH)_4$.